

# Assessment of Retrieved GPS Products Using an Observing System Simulation Experiment

S.-H. Chen<sup>1</sup> and F. Vandenberghe<sup>2</sup>

<sup>1</sup>Land, Air, and Water Resources, University of California, Davis, CA 95616

<sup>2</sup>National Center for Atmospheric Research, Boulder, CO 80305

## 1. Introduction

The bending angle received from low earth orbit satellites (LEO) can be used to derive the refractivity of the atmosphere. However, the information is retrieved under the assumption that the atmosphere is locally spherically symmetric. In general, this assumption has proved to be verified for a global model with moderate resolution (>120km), and assimilating Abelian retrievals as “local” refractivity profile measurements has seemed to be partly successful. This approach, however, is likely to fail with mesoscale models, where the existence of humidity gradients on short distances can severely affect the horizontal homogeneity of atmospheric refractivity. In this presentation, we report a study on the validity of the assumption of the locally spherical symmetry on the retrieved refractivity at mesoscale using an Observing System Simulation Experiment (OSSE) approach.

## 2. Methodology and Experiment Design

With a high resolution of the 5<sup>th</sup> generation of the Penn State/NCAR Mesoscale Model (MM5; Grell et al 1994), we use reanalysis from NCEP Global Data Assimilation System (GDAS) at 00Z July 17 1997 for this study. The horizontal resolution of the MM5 model is 10 km, and the grid intervals are 504 x 504 x 30 in the x-y-z directions. Hurricane Danny, which occurred in July 1997, created an inhomogeneous moisture field over the Gulf of Mexico. This inhomogeneity provides a unique opportunity for studying the assumption of locally spherical symmetry. To recover some moisture deficiency and mesoscale features in the vicinity of Danny in the global reanalysis, SSM/I radiances are assimilated using the MM5 3DVAR system with the first guess from NCEP GDAS data (Chen et al. 2003). This data set is called a perfect data set and will be used for generating observations and for comparison. Figure 1 shows the total column water vapor and 950 mb wind vectors in the Gulf of Mexico. There is a cyclonic circulation and high moisture content in the northwest of the Gulf of Mexico, where Danny is located (black dot).

With the perfect data set, a ray-tracing model is applied to generate a vertical cross section of 2D beams (bending angles) lined in the east-west direction passing through the occultation point A in Fig. 1. Then, the refractivity in column A is retrieved by Abelian inversion of bending angle distributions. The difference of this retrieved refractivity from model local refractivity (perfect refractivity) is quantified.

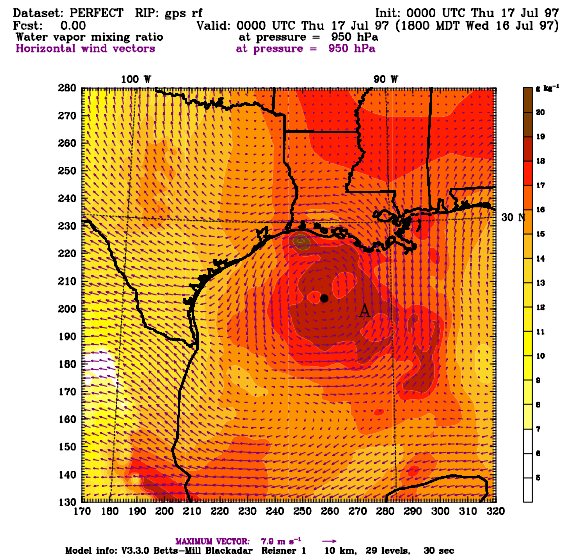


Fig.1: The total column water vapor and 950 mb wind vectors over the Gulf of Mexico are presented. Note that only a small portion of domain is plotted.

## 3. Preliminary Results

Figure 2a shows the vertical profile of perfect refractivity ( $n$ ), which is calculated using the perfect data set, at the occultation point A with the formula:

$$n = 1 + c_1 \frac{P}{T} + c_2 \frac{e}{T^2},$$

where  $P$  is pressure;  $T$  is temperature, and  $e$  is water vapor pressure.  $c_1$  ( $=7.76 \times 10^{-7} \text{ K/Pa}$ ) and  $c_2$  ( $=3.73 \times 10^{-3} \text{ K}^2/\text{Pa}$ ) are constants. The refractivity is about 300 to 400 units in the lower

troposphere and exponentially decreases to 50 to 100 units in the upper troposphere. Figure 2b presents the difference of the vertical profile of the retrieved refractivity from the perfect one in Fig. 2a. The discrepancy can reach 10 units in the lower troposphere. It appears that the retrieved data underestimate the refractivity, and the primary contribution might be from the assumption of locally spherical symmetry. The difference dramatically decreases with heights below 4 km and then slightly increases to the top of the plotted domain.

Since refractivity is a function of pressure, temperature, and water vapor mixing ratio ( $q$ ), the assimilation of retrieved refractivity will directly affect the 3DVAR analysis of those fields (control variables). Therefore, it is an intuitive question to ask how significant the difference of refractivity in the lower troposphere ( $\sim 10$  units; Fig. 2b) is related to these three atmospheric variables ( $p$ ,  $T$ , and  $q$ ), and which of them might play the most important role.

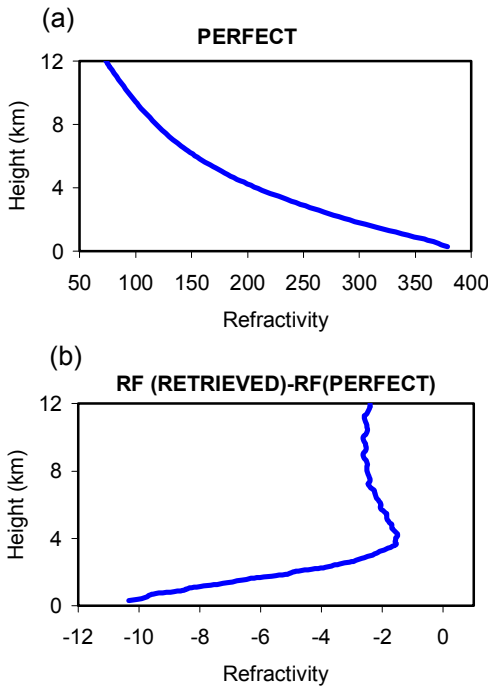


Fig.2: (a) The vertical profile of the refractivity at occultation point A. (b) The difference between the retrieved refractivity and the perfect refractivity.

#### 4. Sensitivity Test

In this section, the sensitivity test of the refractivity with respect to  $P$ ,  $T$ , and  $q$  is examined. The  $P$ ,  $T$ , and relative humidity ( $RH$ )

are perturbed randomly, and the maximum values are 3 hPa, 3 K, and 10 %, respectively. The  $RH$  is perturbed instead of  $q$  because it is easier to control the situation of saturation, which is imposed as a constraint; nevertheless, all figures and discussion are still presented in terms of  $q$ . For each variable, twenty perturbation samples are randomly generated, and every two are paired with the same magnitude but different signs except for the moisture field. In the situation of saturation, the perturbation is cut down to a value that the total  $RH$  exactly reaches 100%. Therefore, the mean values of  $P$  and  $T$  perturbations are zero, while some small negative averaged values for the  $q$  perturbation are obtained at the height of about 1 ~ 2.5 km due to saturation.

Figure 3 shows the vertical profile of root mean square values (RMSs) from 20 perturbation samples for pressure (dotted line), temperature (long-dashed line), and water vapor mixing ratio (solid line). The RMSs are about 1.5 ~ 2 for pressure (hPa) and temperature (K) in the whole column. However, the vertical profile for  $q$  is significantly different from other two since the saturation-mixing ratio dramatically decreases with height due to the temperature distribution.

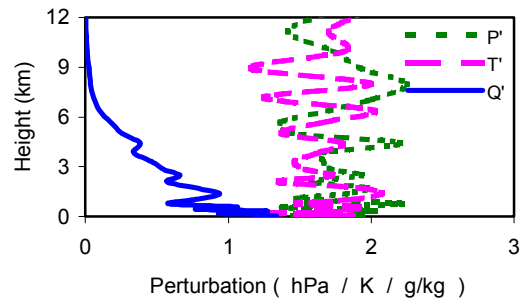


Fig.3: The averaged root mean square values of pressure perturbation (hPa; dotted line), temperature perturbation (K; long-dashed line), and mixing ratio perturbation ( $g\ kg^{-1}$ ; solid line).

Four cases are conducted to examine the variation of refractivity after three variables are perturbed at the same time (one case) or an individual variable is perturbed (3 cases), and results are shown in Figure 4. The refractivity in the lower troposphere is highly sensitive to these perturbations, and the variation of refractivity can be over 10 units (Fig. 4a). More precisely, it is found that the primary contribution to these refractivity variations is from the moisture field (Fig. 4d vs. Figs 4c and 4b), whose influence can be 10 times of that of the pressure perturbation in

our setup. The contribution of the temperature perturbation can also be important in the lower troposphere (20 % of that from the moisture perturbation). It is worth mentioning that these perturbed values used in this study are reasonable and comparable to some observational errors or errors imbedded in the model initial field. In addition, the variation of the refractivity after perturbing the three variables (or the moisture variable only) is comparable to the refractivity error due to the symmetric assumption in the retrieval algorithm (Fig. 2). This implies that after assimilating retrieved refractivity, the errors of the  $P$ ,  $T$ , and  $q$  fields in the 3DVAR analysis might be comparable to errors in the model initial condition, and we have learned that those errors can lead to significant model forecast uncertainty.

### 5. Concluding Remarks

Using a high-resolution mesoscale model with an Observing System Simulation Experiment (OSSE) approach, it is found that retrieved refractivity might be underestimated and its uncertainty in the lower troposphere can reach about 10 units under the assumption of locally spherical symmetry. From a sensitivity study, we also found that refractivity is very sensitive to the low-level moisture field and to a lesser extent, the low-level temperature field. Both findings provide possible evidence that assimilating retrieved refractivity might introduce errors in pressure, temperature, and moisture in the 3DVAR analysis, and these errors are comparable to errors imbedded in the mesoscale model initial condition, which might lead to significant uncertainty in a high-resolution mesoscale model forecast.

In the next step we will study the assimilation of retrieved refractivity and perfect refractivity, and compare the impact of these two sets of data on high-resolution mesoscale model simulations and forecasts.

**Acknowledgements:** The authors would like to thank the MM5 3DVAR group. The SSM/I data were provided by the Global Hydrology Resource Center at the Global Hydrology and Climate Center, NASA, Huntsville, Alabama.

### References

Grell, G. A., J. Dudhia, and D. R. Stauffer, 1994: *A description of the fifth-generation Penn State/NCAR mesoscale model (MM5)*.

NCAR/TN-398+STR, National Center for Atmospheric Research, Boulder, CO, 122 pp.  
 Chen, S.-H., F. Vandenberghe, G. W. Petty, and J. F. Bresch, 2003: Application of SSM/I satellite data to a hurricane simulation, submitted to *Quart. J. Roy. Meteor. Soc.*, under revision.

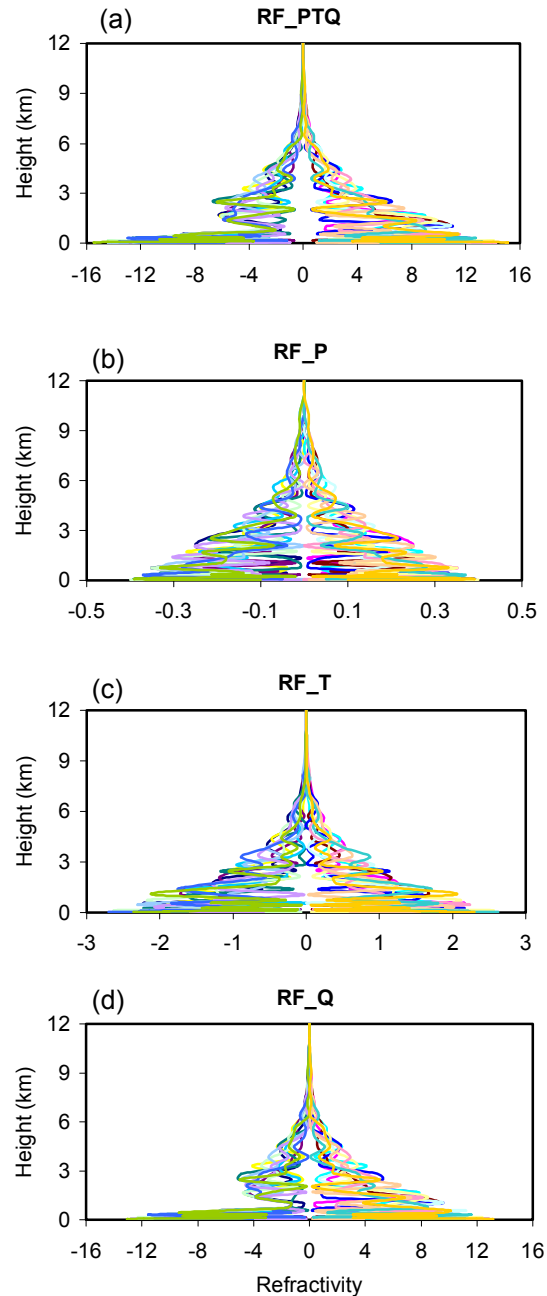


Fig.4: The difference of refractivity from the perfect data after perturbing (a) pressure, temperature, and moisture, (b) pressure only, (c) temperature only, and (d) relative humidity only. Twenty samples are plotted.

